

Calibration of two-dimensional variably saturated numerical model for groundwater flow in arid inland basin, China

Xiaomin Gu, Jingli Shao*, Yali Cui and Qichen Hao

Alluvial fan is an important recharge area for arid and semi-arid inland basins. In order to study groundwater circulation and quantify recharge amount of the groundwater system in arid inland basins, it is necessary to use numerical models. In this study, a 2D variably saturated numerical model of a typical profile has been developed using EOS 9 module of TOUGH2. The mesh for the fine soil plain area was refined compared with previous studies and the minimum cell size was 0.1 m in thickness. An improved approach in TOUGH2 was applied to calculate the groundwater evapotranspiration more efficiently and characterize water transport more accurately. Multiple calibration approaches were combined to calibrate the model. The results show that, the typical profile can be divided into three groundwater flow systems. The circulation depth for the local groundwater flow system is about 200 m and the shallow discharge accounts for 74.4% of the total amount with groundwater age less than 500 a (year). The circulation depth for the middle flow system can reach 800 m and the amount of discharge accounts for 18.5% of the total amount with groundwater age less than 10 ka (kiloyear). The circulation depth for the regional flow system is from 1000 to 1500 m, and the discharge accounts for 7.1% of the total amount with groundwater age ranging from 10 to 50 ka. The improved TOUGH2 numerical model, combined with multiple calibration approaches, can better reflect regional circulation characteristics and quantify the recharge amount of different groundwater sub-systems in arid and semi-arid inland basins with limited datasets.

Keywords: Arid inland basin, groundwater flow, numerical models, multiple calibration approaches.

GROUNDWATER is an important and major source of drinking water worldwide and the sole water source for many countries. Alluvial fan, which has high porosity and substantial thickness, is the main recharge area for arid and semi-arid inland basins. Therefore, a thorough understanding of recharge and flow paths in alluvial aquifers is necessary for water resource management as well as sustainable utilization of local and regional groundwater resources^{1,2}.

Numerical modelling provides an efficient method for identifying the flow path and dynamics of groundwater, as well as quantifying the recharge from different sources³. Previous studies indicated that evapotranspiration is an important hydrological factor influencing groundwater system in arid and semi-arid regions. For areas with shallow water table, evapotranspiration is

greatly affected by phreatic fluctuations related to the weather, temperature, soil moisture, etc. Thus, it is necessary to establish a coupling model in variably saturated zone to study groundwater circulation^{4,5}. In the present study, TOUGH2 (Transport of Unsaturated Groundwater and Heat 2) is used to develop a variably saturated model. It is a numerical simulator for non-isothermal flows of multicomponent, multiphase fluids in two- and three-dimensional porous and fractured media⁶. It has been widely used in nuclear waste disposal, geothermal reservoir engineering, CO₂ storage⁷, unsaturated and saturated zone hydrology⁸, and other fields⁹.

In order to describe the characteristics of the profile along the alluvial plain in arid inland basins, a two-dimensional variably saturated numerical model has been developed. Meanwhile, the impact of evapotranspiration on the groundwater flow system is also considered. However, the reliability of the recharge estimated depends on the conceptual model, as well as the discrete spatial and hydraulic parameters. With limited datasets in arid inland basins^{10,11}, multiple calibration approaches are used to calibrate the model. Liu *et al.*³ used natural stable

Xiaomin Gu, Jingli Shao and Yali Cui are in the School of Water Resources and Environment, China University of Geosciences, Beijing 100083, P.R. China; Qichen Hao is in the Institute of Hydrogeology and Environmental Geology, Chinese Academy of Geological Science, Shijiazhuang 050061, P.R. China.

*For correspondence. (e-mail: jshao@cugb.edu.cn)

isotopes as additional calibration targets to simulate the distribution of groundwater recharge in an alluvial aquifer system in Japan. The combined use of isotopic approach eliminated the errors due to limited data and provided a better understanding of the groundwater recharge mechanism. Dahan *et al.*¹² combined a multi-variable mixing cell model with MODFLOW model to simulate the hydrochemical and hydrogeological model. The parallel application of two approaches provides an excellent tool for the validation of the model. Sanford *et al.*¹³ used the available hydrochemical data to calibrate the model parameters and recharge rates. The errors of the calibrated model were smaller than those used in previous models.

In this study, a 2D variably saturated numerical model has been developed using TOUGH2 software. The trial and error method, particle tracking and isotopic dating methods were combined to calibrate the model. The study not only provides insight into the calibration of two-dimensional variably saturated groundwater flow model, but also provides effective methodologies for preliminary estimation of regional groundwater circulation and flow systems with limited datasets¹⁴.

Study area

The Qaidam basin, one of the largest inland basins in China, is formed by various alluvial fans. The study area is one of the typical alluvial fans in Qaidam basin, including Nomhon alluvial fan (NAF) and Amunick alluvial fan (AAF) (Figure 1). The specific yield values for the study area are estimated by Hao *et al.*¹⁵. The annual mean precipitation is 43 mm, and approximately 68% of this occurs during the wet season from June to August according to climatic normal (1978–2014). The annual mean temperature in the area is 5°C. The potential evapotranspiration was estimated using Thornthwaite method¹⁰ and the annual mean potential evapotranspiration was worked out to be 2600 mm in the study area.

The typical profile extends from the top of the Nomhon alluvial fan to Amunick Mountains (Figure 1). The simulated profile is 100 km long and the longitudinal (Z direction) extent is 2100 m. Two independent groundwater subsystems (Amunick groundwater system and Nomhon groundwater system) exist in the study area (Figure 2). AAF is located in the northern part of the study area at an altitude ranging from 2780 to 2890 m and its construction is similar to NAF. The groundwater flow of NAF runs from south to north.

The alluvial aquifers in the study area mainly consist of gravel and sand, and the aquitard is composed of pumice and clay (Figure 2). The northern part of the study area is a fine soil plain with a flat terrain (alluvial lacustrine plain) with altitude ranging from 2700 to 2720 m. From the piedmont to the fine soil plain, the aquifer

structure changes from a single phreatic to a multilayer structure, and the depth to groundwater level also decreases. The fine soil plain area is a discharge area.

Agricultural and residential areas, and deserts are the three major land-cover types in the study area. Most of the agricultural and residential areas are distributed upstream. The irrigation season usually begins in June and ends by August. The groundwater of the alluvial fan is abstracted for local use and there are no large water consumption wells found in the study area for agricultural and industrial use. As a result, groundwater abstraction is estimated to be extremely small and has no significant influence on the groundwater flow system in the study area.

Methods

Sampling and analysis

Field works were conducted in 2014 during May to July. The groundwater samples were collected from wells and springs for analysing ³H and ¹⁴C to determine groundwater age. Tritium content was determined by electrolytic enrichment and liquid scintillation technique. The measurement accuracy was ±0.3 Tritium Unite (TU). Activity of ¹⁴C was analysed by accelerator mass spectrometry and standard deviation of the analytical results ranged between 0.7 and 1.0 pMC (percentage of modern carbon). Water table of the sampling wells was also measured during the period. Observation equipment consisted of mainly divers and water-level recorders. In some regions, there were no monitoring instruments.

Model description and construction

The well-established software code TOUGH2 was used for modelling groundwater flow in the study area. The 2D variably saturated model was developed using EOS9 module to describe water flow under partially saturated and fully saturated conditions, as well as phase changes between the two. The control equation is¹⁶

$$\sigma(h) \frac{\partial h}{\partial t} - \nabla[K(h)\nabla(h+z)] = q, \quad (1)$$

where t is the time (sec), h the pressure head (m), z the elevation (m), $\sigma(h)$ the specific storage, $K(h)$ the unsaturated hydraulic conductivity (m/d) and q is the source/sink.

The conceptual model was developed according to hydrogeological conditions as accurately as possible to be effectively represented in the computation grid. The spacing between boreholes ranged between 5 and 20 km; and hence, we adopted a cell size of 1 km, smaller than the minimum distance between the boreholes. In order to accurately describe the characterization of the variably saturated

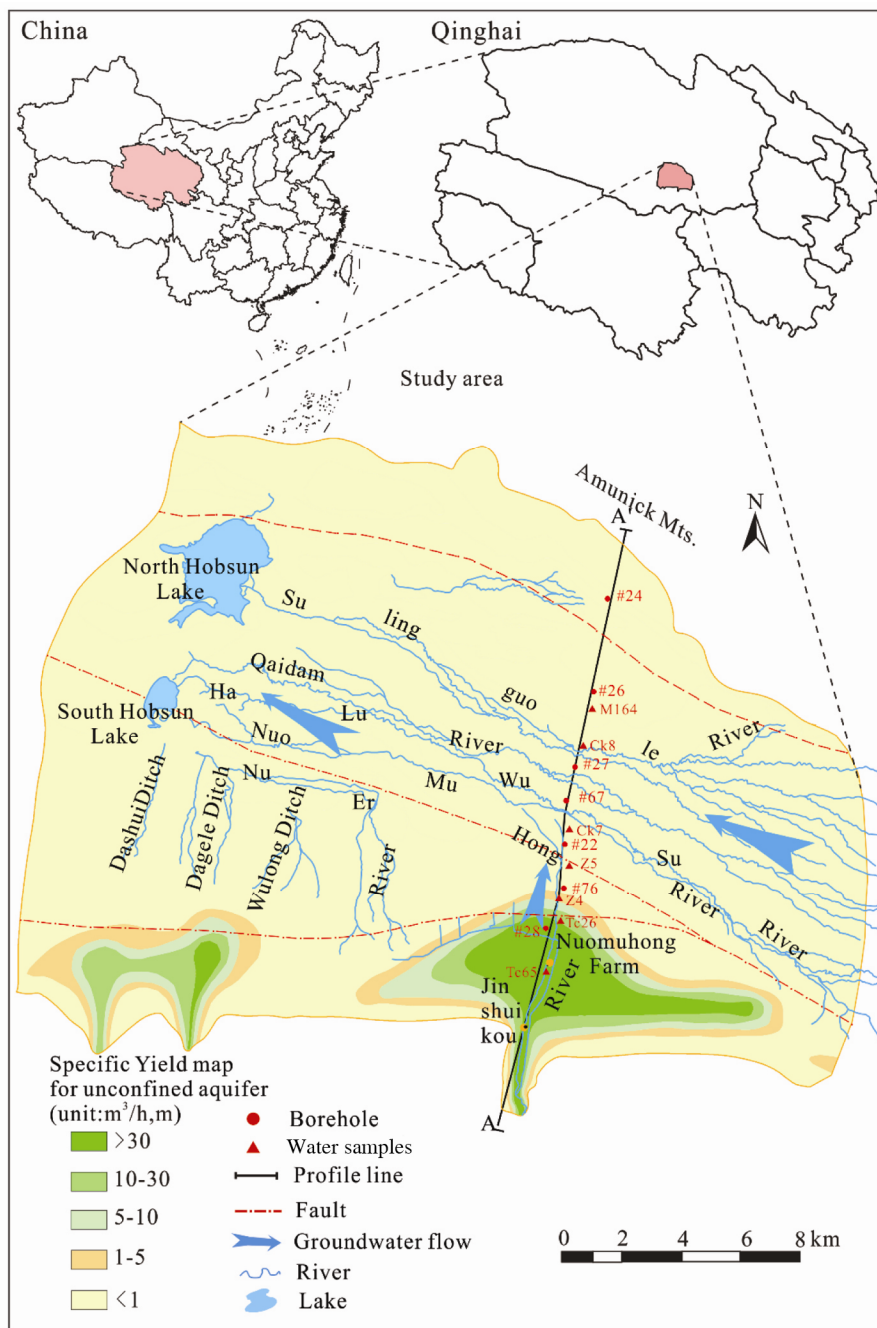


Figure 1. Overview of the study area.

zone, cell thickness should be as small as possible, which leads to an increase in the cell number and simulation time. Thus, in order to decrease the cell number and run the simulation model efficiently, an irregular gradient discretization method was applied¹⁵. The minimum cell size was 0.1 m in thickness. The total number of grids was 3150 and the total number of connections between cells was 6187.

The piedmont area is generalized into a sand and gravel aquifer, and the fine soil plain area is generalized as an interbedded clay and sand structure. According to

the hydraulic conditions in the study area, the groundwater system remains in dynamic equilibrium with a small amount of groundwater exploitation (50–200 m³/a). Therefore, a steady groundwater flow model was developed.

Parameter setting

The hydraulic parameters, including lithological and hydrodynamic parameters, reflect regional hydraulic structure as well as the distribution of sources and sinks¹⁷. Table 1 lists the hydraulic parameters used in this model.

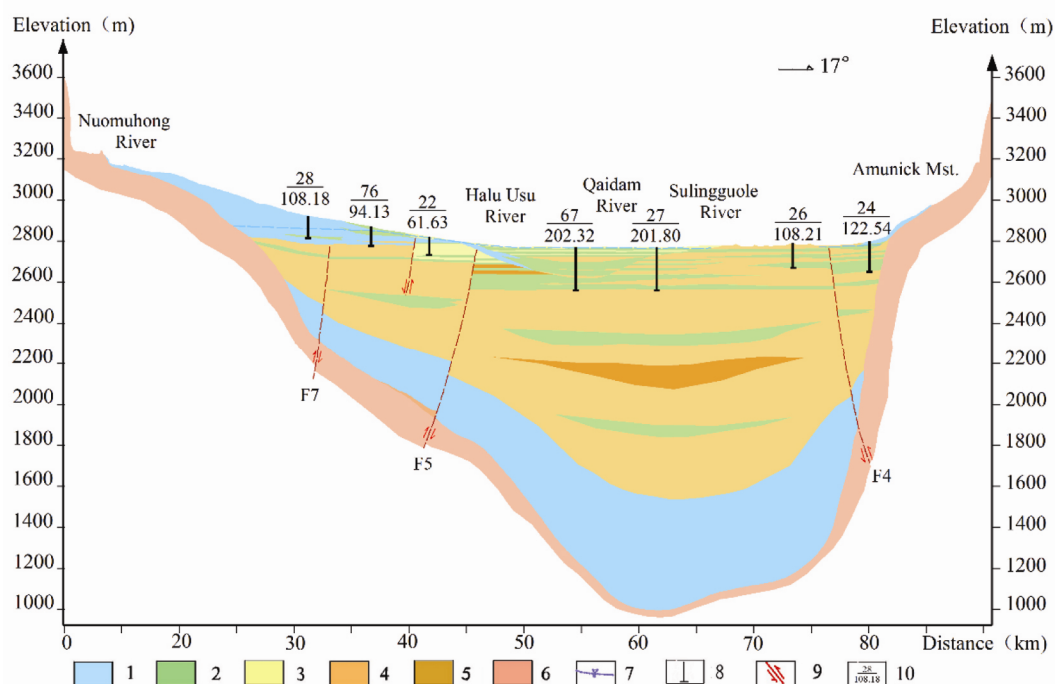


Figure 2. Hydrogeological profile view (A–A'). 1, Sand gravel; 2, Sand; 3, Silt; 4, Silty clay; 5, Clay; 6, Bedrock; 7, Phreatic level; 8, Borehole; 9, Fault; 10 (Borehole number/depth of holing).

Table 1. Parameters and empirical value of the model

Hydraulic parameters	Parameter definition	Value
Lithological parameters	ρ_s : The density of rock particles, associated with liquid flow rates	1400 kg/m ³
	μ : Diffusion coefficient, the ability of solute transport in solution	0.155e-02 Pas
	PI: Productivity index, the capacity of flow overcoming resistance and rising to the surface	4.00e-10 m ³
Hydrodynamic parameters	k : Permeability, the capacity of rock permeability	(10 ⁻² –10 ⁻³) m/d
	ϕ : Porosity, water storage and performance characterization of rocks	0.3
	E_{ms} : Potential evaporation, the capacity of soil evaporation	2000 mm·a ⁻¹
	S_{lr} : Liquid residual moisture content, bound water moisture for dry soil	0.15
	S_{ls} : Saturated liquid water content (use default value)	1.00

The initial value of the first two parameters is given based on empirical values, while other parameters are determined by laboratory test and corrected using the empirical values. The lithologic units occurring in the hydrogeologic profile were assigned to the corresponding grid cells using the following approximations (Figure 2):

- (1) Since the profile depends on the lithology of boreholes, an error inherited is in lithological identification that is a function of workers' biased judgements and is impossible to remove. Therefore, the profile was used directly in the conceptual model to maintain a comparable degree of approximation in actual hydrogeologic conditions. Six different hydrogeologic units have been identified to represent the lithologies' characteristics. These are sand gravel, sand, silt, silty clay, clay and granite.

- (2) The hydrogeologic units were manually assigned to cells using ArcGIS 10.0. The coordinate of cell centre was extracted and registered with the profile; the lithologies of the profile were assigned to the cells.

Sources and sinks

Groundwater recharge sources include precipitation infiltration, lateral inflow, river and canal leakage, among which river leakage is the main recharge source. The model showed constant flow conditions on both sides of the piedmont region, where it is recharged by river seepage and lateral inflow. The recharge rate was 11,200 m³ a⁻¹, according to Darcy's section method. The recharge rates were assigned as constant head boundaries using GENER code in the model. The bedrock was generalized as an impermeable boundary. The springs and rivers were simulated as

a sink term of groundwater using mixed boundary and the surface as an evapotranspiration boundary.

Soil evapotranspiration is not only affected by climate and weather factors, but is also associated with soil moisture. According to previous studies, formulae for topsoil moisture calculation have been summarized by Rui¹⁸, indicating different quantitative laws for soil evapotranspiration during different processes and revealing the relationship between evapotranspiration ratio and soil moisture content. TOUGH2 defines evapotranspiration as source and sink terms without considering the impacts of weather, temperature, soil moisture and other factors at a certain timescale. Therefore, computational methods for the topsoil moisture equation (eq. (2)) were used for improving the source for TOUGH2. The equation was developed based on surface soil moisture content. Evapotranspiration was considered as a function of soil saturation given as an upper boundary to characterize water transport near the surface through iterative calculation. The improved evapotranspiration upper boundary can calculate the groundwater evapotranspiration more efficiently and characterize water transport more accurately in variably saturated flow modelling¹⁵

$$E_s = \begin{cases} E_{ms}, \theta \geq \theta_f \\ \frac{E_{ms}}{\theta_f}, \theta_m \leq \theta \leq \theta_f, \\ CE_{ms}, \theta < \theta_m \end{cases} \quad (2)$$

where E_s is the soil evapotranspiration (kg/s), E_{ms} the potential soil evapotranspiration (kg/s), θ the soil moisture content, θ_f the field capacity, θ_m the capillary rupture moisture and C is the evapotranspiration coefficient for soil moisture content less than θ_m , which is far less than 1.

Model calibration

Groundwater level calibration: The model calibration was quantitatively assessed by calculating the determination coefficient (R^2) and root mean square error (RMSE) of the simulated and observed hydraulic heads^{19,20}. The statistical measures are

$$RMSE = \frac{\sqrt{\sum_{i=1}^k (H_{Si} - H_{Oi})^2 / k}}{H_{Om}}, \quad (3)$$

$$R^2 = \left(\frac{\sum_{i=1}^k (H_{Oi} - H_{Om})(H_{Si} - H_{Sm})}{\sqrt{\sum_{i=1}^k (H_{Oi} - H_{Om})^2 \sum_{i=1}^k (H_{Si} - H_{Sm})^2}} \right)^2, \quad (4)$$

where H_{Si} is the simulated hydraulic head, H_{Oi} the observed hydraulic head, H_{Om} the mean observed hydraulic head and H_{Sm} is the mean simulated hydraulic head.

Groundwater age calibration: In order to simulate groundwater flow transport, the particle tracking method²¹ and linear interpolation were used to obtain the particle velocity, calculate residence time and position of the particle motion, and then, simulate groundwater age distribution in the aquifer. The Tecplot visualization software was used to plot the simulation results and draw the contours of groundwater age, which were corrected using isotopic dating data.

Partial differential equation for a stable three-dimensional groundwater flow system can be expressed as

$$\frac{\partial}{\partial x}(\phi v_x) + \frac{\partial}{\partial y}(\phi v_y) + \frac{\partial}{\partial z}(\phi v_z) = w, \quad (5)$$

where v_x , v_y and v_z are the three components of the groundwater velocity (m/d); ϕ the porosity and w is the unit volume of water consumed or generated by internal sources or sinks. Equation (5) is a mass conservation equation for an infinitesimal volume of the aquifer; its finite difference can be approximated as mass conservation equations for finite volume of the aquifer.

Results and discussion

Groundwater level calibration

The model identification results indicate that the simulated hydraulic heads fit well with the observed hydraulic heads which is an important evaluation index for the simulated reality²². The lack of systematic observations makes it difficult to simulate groundwater level fluctuation accurately and quantitatively over time. In this study, 52 monitoring data points for mean groundwater level were used for model correction. By constantly adjusting the boundary conditions, the hydraulic parameters and the source and sink terms get the best fit of the observed hydraulic heads and simulated hydraulic heads.

Figure 3 shows a comparison chart of simulated and measured hydraulic heads after parameter calibrations. R^2 is 0.9; the maximum and minimum errors are 4.9 and 0.21 m respectively; the mean absolute error is 0.36 m, and RMSE is 1.85 m. Regions with larger errors are mainly concentrated in the piedmont area due to lack of data, and the parameters are determined by empirical values; thus, certain errors and uncertainties may exist in the groundwater level calibration. Simulated and measured hydraulic heads fit better in the fine soil plain area, with an error between 0.2 and 1.5 m. The error is mainly caused by heterogeneity and anisotropy in the lithology.

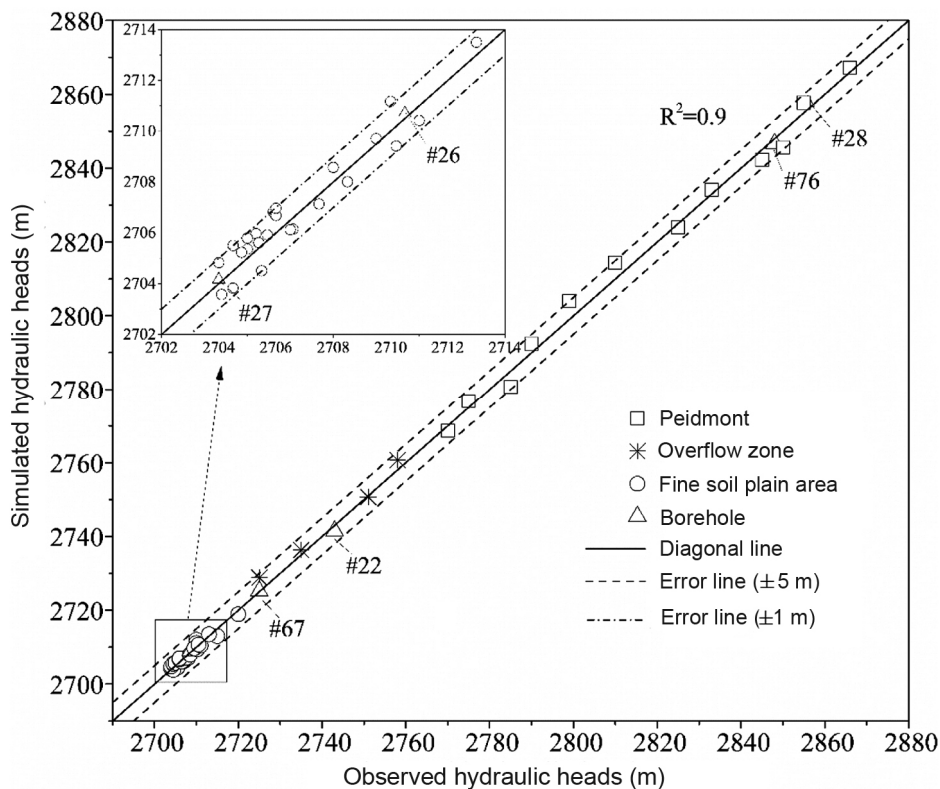


Figure 3. Comparison chart of measured and simulated water level.

Table 2. Error calculation table for a typical borehole

	Well no.						Mean error	Mean absolute error
	#28	#76	#22	#67	#26	#27		
Error (m)	1.74	-1.32	0.29	-0.21	0.17	0.42	0.16	0.69

Table 3. Trial-and-error result of rock parameters

Lithology	Porosity	Equivalent permeability coefficient (m/d)		
		X	Y	Z
Sand and gravel	0.3	50.02	50.02	5.17
Sand	0.35	14.63	14.63	2.01
Silt	0.5	0.65	0.65	0.12
Silty clay	0.65	0.03	0.03	0.003

Leakage flow in the aquitard increases the vertical flow to a certain degree²³.

Table 2 shows calculation errors for the six typical boreholes (observation wells), which are evenly distributed along the profile (Figure 1). Well nos 28 and 76 are located at the leading edge of the alluvial fan, #22 at the overflow area, #67 and #27 near the centre of the Qaidam River and #26 north of Sulinguole River. The mean absolute error for the six observation wells is 0.69 m, which is well fitted. Well nos 28 and 76, which are located in the

piedmont region, lack a control point. The simulation error is larger than the observation wells in the overflow area and centre of the basin, where the error is less than 0.5 m.

Parameter calibration

Table 3 shows results from the parameter identification. Since a sand mezzanine exists in the aquitard, the parameters obtained from the model are greater than the empirical parameters. The permeability coefficients of silt and silty clay are generalized into an equivalent permeability coefficient. During the process of model identification, the simulated hydraulic heads are higher than the measured ones, which indicates that the presence of sand mezzanine in the aquitard would change the groundwater flow mode and place of discharge. As a result, sand mezzanine should be taken into consideration when dividing the groundwater flow systems.

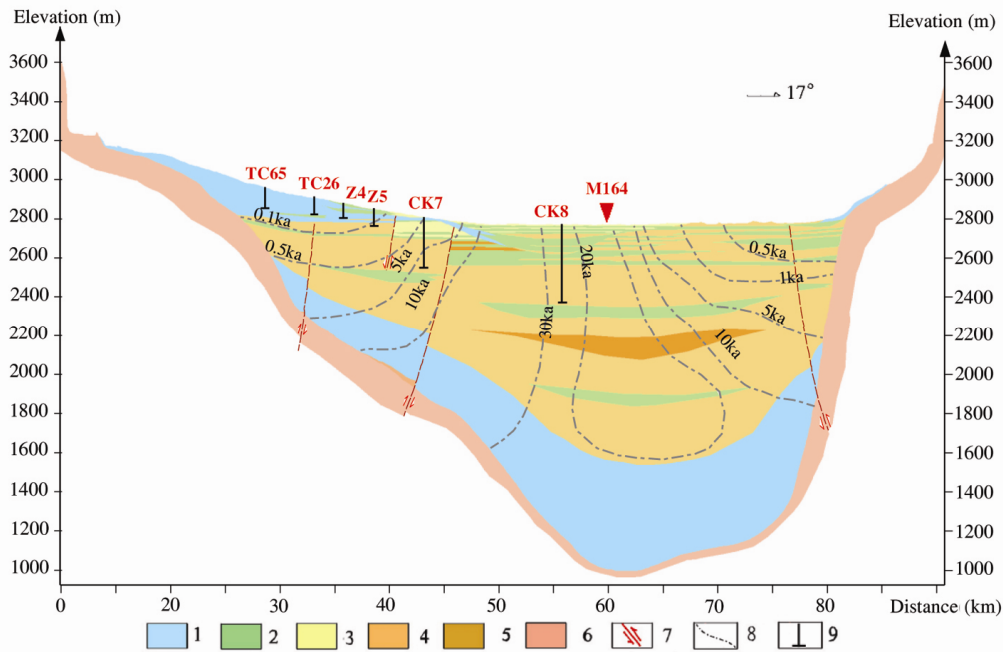


Figure 4. Groundwater age contours of a typical profile in Nomhon alluvial fan. 1, Sand and gravel; 2, Sand; 3, Silt; 4, Silty clay; 5, Clay; 6, Bedrock; 7, Fault; 8, Groundwater age contours; 9, Isotopic dating borehole.

Table 4. Comparison of simulation age and isotopic dating results

Sample	TC65	TC26	Z4	Z5	CK7	CK8	M164
Isotopic dating results (a)	16	22	18	1,100	5,000–10,000	21,000	28,000
Simulation age (a)	<100	<100	<100	200	6,000	22,000	30,000

Table 5. Groundwater balance of the study profile

Water balance		Amount (m ³ a ⁻¹)	Proportion (%)
Recharge	Recharge from southern piedmont	8,819.36	79.0
	Recharge from northern piedmont	2,344.39	21.0
	Total amount	11,163.744	100.0
Discharge	Evaporation	3,845.38	34.4
	Spring overflow	6,948.16	62.2
	River discharge	54.83	0.5
	Lateral run-off discharge	315.36	2.8
	Total amount	11,163.724	100.0
Error		-0.020	

Calibration of groundwater age

To further validate the calibration results, groundwater age contours (Figure 4) were drawn to compare with ¹⁴C and ³H isotopic dating results (Table 4). The groundwater flow results from the TOUGH2 output file have been used to draw groundwater age contours using the Tecplot software.

Figure 4 shows that at the same location in the study area, the groundwater age in the shallow area is younger than that in the deep area, and increases along the direc-

tion of groundwater streamline. Groundwater is usually mixed and its age is an interval value due to dispersion, adsorption and ion exchange during the migration processes²⁴. The Sulingguole River is the position of the final groundwater drainage, and the age of groundwater is about 30 ka. Water samples from TC65, TC26, Z4 are modern water, and isotopic dating results are less than 100 year, which is in agreement with the simulation results. Simulation results for groundwater age at CK8 and M164 are about 22 and 30 ka, fitting well with isotopic dating results of 21 and 28 ka respectively. Therefore, the numerical simulation results are highly reliable, and can be used as an important method to evaluate the groundwater flow system in the study area.

Water balance analysis

Table 5 provides the results of water balance. The groundwater recharge is 11,163.74 m³ a⁻¹, consisting of 79% from the southern piedmont and 21% from the northern piedmont. Spring overflow is the main form of discharge, accounting for 62.2% with an amount of 6948.16 m³ a⁻¹, while evapotranspiration accounts for 34.4% of the total amount, about 3845.38 m³ a⁻¹. River

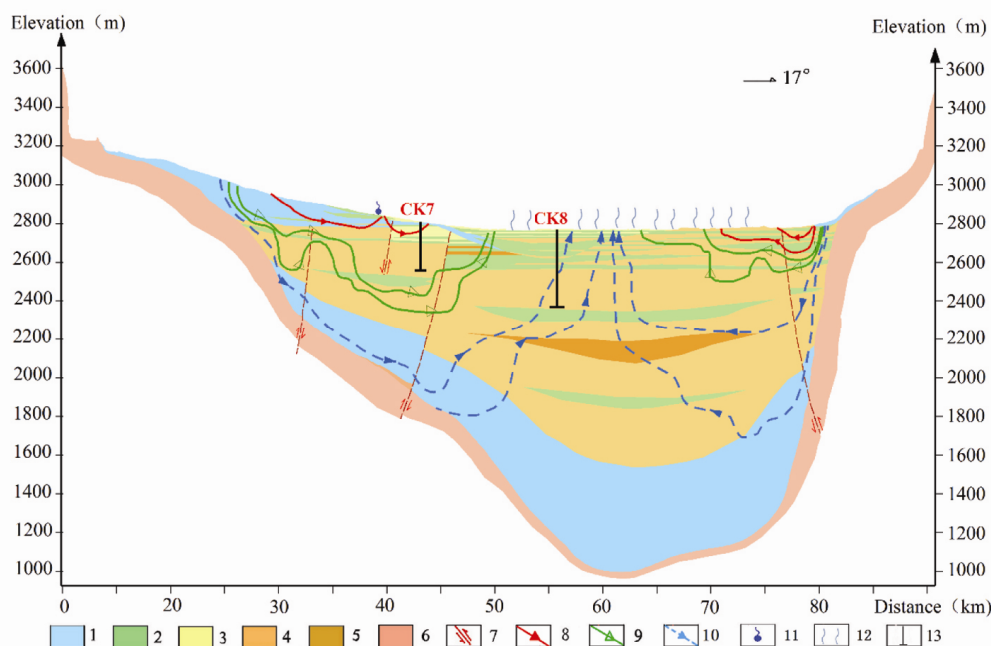


Figure 5. Groundwater streamlines of a typical profile in Nomhon alluvial fan. 1, Sand and gravel; 2, Sand; 3, Silt; 4, Silty clay; 5, Clay; 6, Bedrock; 7, Fault; 8, Streamlines for the local groundwater flow system; 9, Streamlines for the middle groundwater flow system; 10, Streamlines for the regional groundwater flow system; 11, Spring; 12, Surface evaporation; 13, Borehole.

discharge mainly consists of: (1) the northern Halu Ussuri River and Sulingguole River with an amount of $54.83 \text{ m}^3 \text{ a}^{-1}$, accounting for 0.5% of the total amount; and (2) the westward Qaidam River, which eventually remits into South Hobson Lake, with an amount of $315.36 \text{ m}^3 \text{ a}^{-1}$, accounting for 2.8% of the total amount. The groundwater equilibrium difference is $0.02 \text{ m}^3 \text{ a}^{-1}$ and the groundwater system is under a state of dynamic equilibrium, filling emission balances.

Cyclic pattern of groundwater system

Based on the groundwater flow output file from TOUGH2 and Tecplot processing software, the groundwater flow chart was obtained (Figure 5). The division of the groundwater flow system can be combined with the terrain²⁵, deposition conditions and hydrogeological parameters²⁶. The groundwater flow characteristics of the profile can reveal the characteristics of vertical circulation and evolution for groundwater systems, determine the form of recharge, and calculate the amount of recharge sources for each system. Figure 5 shows the basin having two independent groundwater flow systems. The potential sources are the southern and northern piedmonts and the central basin is the potential sink. The typical profile can be divided into three groundwater flow systems – local, middle and regional.

The local groundwater flow systems originate from the top of the piedmont alluvial fan to the Halu Ussuri River

and the region between the north piedmont plain and the Sulingguole River. The springs are exposed near the overflow area. The longitudinal impact width of the local groundwater system ranges from 10 to 20 km. The circulation depth is about 200 m and the age of the groundwater is generally less than 500 a; Qaidam River is the boundary of the middle groundwater flow system. Salient groundwater streamlines are affected by the buried fault, which has a longitudinal impact width of about 30–40 km. Its circulation depth can reach 800 m. Groundwater age is generally less than 10 ka, and it changes with the different lithology and groundwater formation conditions of the regions. The groundwater recharge from the northern and southern piedmonts and discharge to the centre of the basin, which constitutes the regional groundwater flow system, has largest longitudinal impact, usually more than 60 km. Its circulation depth reaches the bottom boundary of the lower Pleistocene stratigraphy, ranging from 1 to 1.5 km. The groundwater age ranges from 10 to 50 ka. Due to the small amount of recharge in the northern piedmont and difference in lithology, the groundwater flow path of AAF is shorter but takes more time than NAF.

By analysing groundwater streamlines combined with drainage location and groundwater ages, the distribution area of three groundwater systems in the simulation profile has been identified. The amount of discharge of the three groundwater flow systems can be calculated using the total amount of discharge estimated in each cell (Table 6). Discharge of the local groundwater flow

Table 6. Calculation of discharge amount in groundwater flow system

Groundwater flow system	Evaporation ($\text{m}^3 \text{a}^{-1}$)	Spring overflow ($\text{m}^3 \text{a}^{-1}$)	River drainage ($\text{m}^3 \text{a}^{-1}$)	Total amount ($\text{m}^3 \text{a}^{-1}$)	Proportion (%)
Local groundwater system	1352.90	6937.86	17.23	8307.98	74.4
Middle groundwater system	2017.35	10.30	37.55	2065.20	18.5
Regional groundwater system	475.13	–	315.40	790.54	7.1

system is $8307.98 \text{ m}^3 \text{a}^{-1}$, accounting for 74.4% of the total amount, with spring overflow being the main form of discharge. The discharge of the middle flow system is $2065.20 \text{ m}^3 \text{a}^{-1}$, accounting for 18.5% of the total amount. Evapotranspiration and spring overflow are the main mode of discharge. The discharge of the regional flow system is $790.54 \text{ m}^3 \text{a}^{-1}$, accounting for 7.1% of the total amount. Evapotranspiration is the most important form of discharge. The local groundwater flow system has a strong renewal capacity, fast circulation speed, and maximum discharge. The groundwater discharge declines through continuous evapotranspiration and lateral discharge in the aquifer. The discharge of the regional groundwater system accounts for only 7% of the total amount.

Conclusion

Employing the improved TOUGH2 numerical simulation software, a two-dimensional variable saturated groundwater flow model of a typical profile has been developed. In this model, complex upper boundaries are considered, such as potential evapotranspiration and water content at the surface. Based on previous studies, vertical simulation depth is increased and the mesh for the fine soil plain is refined in order to accurately calculate the surface evapotranspiration discharge and study the deep circulation of groundwater flow systems.

Multiple calibration approaches have been combined to calibrate the model. The groundwater level calibration results show that R^2 is 0.9; the mean absolute error and RMSE are 0.36 and 1.85 m respectively. The simulation results fit well with the measured data. The groundwater age calibration results show that the simulation results of groundwater age are in agreement with the isotopic dating results. Therefore, the numerical simulation results are highly reliable. The circulation depth for the local groundwater flow system is about 200 m and shallow discharge accounts for 74.4% of the total amount with groundwater age less than 500 a. The circulation depth for the middle flow system can reach 800 m and discharge accounts for 18.5% of the total amount with groundwater age less than 10 ka. The circulation depth for the regional flow system is from 1000 to 1500 m and the discharge accounts for 7.1% of the total amount with groundwater age ranging from 10 to 50 ka.

The TOUGH2 numerical simulation along with isotopic dating correction methods reflect recycling charac-

teristics of the regional groundwater flow system, and have a certain significance to the preliminary estimation of regional groundwater circulation and flow systems with limited datasets. The pattern of groundwater flow system has been established, and the groundwater recharge rate is specified as a form of steady flow without considering the effects of temporal and spatial variation. In future studies, different recharge sources and recharge forms should be taken into consideration to explore their effects on the flow system. In addition, solute transport methods which consider the effects of dispersion and density changes can be combined with the model.

- Choi, B. Y., Yun, S. T., Mayer, B., Chae, G. T., Kim, K. H., Kim, K. and Koh, Y. K., Identification of groundwater recharge sources and processes in a heterogeneous alluvial aquifer: results from multi-level monitoring of hydrochemistry and environmental isotopes in a riverside agricultural area in Korea. *Hydrol. Process.*, 2010, **24**(3), 317–330.
- Liu, F., Cui, Y.-l., Zhang, G., Geng, F. and Liu, J., Using the ^3H and ^{14}C dating methods to calculate the groundwater age in Nomhon, Qaidam Basin. *Geoscience*, 2014, **28**(6), 1322–1328.
- Liu, Y., Yamanaka, T., Zhou, X., Tian, F. and Ma, W., Combined use of tracer approach and numerical simulation to estimate groundwater recharge in an alluvial aquifer system: a case study of Nasunogahara area, central Japan. *J. Hydrol.*, 2014, **519**(Part A), 833–847.
- Scanlon, B. R., Healy, R. W. and Cook, P. G., Choosing appropriate techniques for quantifying groundwater recharge. *Hydrogeol. J.*, 2002, **10**(1), 18–39.
- Zhu, Y., Shi, L., Yang, J., Wu, J. and Mao, D., Coupling methodology and application of a fully integrated model for contaminant transport in the subsurface system. *J. Hydrol.*, 2013, **501**, 56–72.
- Xu, T., Sonnenthal, E., Spycher, N. and Pruess, K., TOUGHREACT: A simulation program for non-isothermal multiphase reactive geochemical transport in variably saturated geologic media. *Comput. Geosci.*, 2006, **32**(2), 145–165.
- Audigane, P., Chiaberge, C., Mathurin, F., Lions, J. and Picot-Colbeaux, G., A workflow for handling heterogeneous 3D models with the TOUGH2 family of codes: applications to numerical modeling of CO_2 geological storage. *Comput. Geosci.*, 2011, **37**(4), 610–620.
- Kuang, X., Jiao, J. J., Li, W., Wang, X. and Mao, D., Air and water flows in a vertical sand column. *Water Resour. Res.*, 2011, **47**(4), 289–306.
- Hubschwerlen, N., Zhang, K., Mayer, G., Roger, J. and Vialay, B., Using Tough2-MP on a cluster-optimization methodology and study of scalability. *Comput. Geosci.*, 2012, **45**, 26–35.
- Hamed, Y. *et al.*, Use of geochemical, isotopic, and age tracer data to develop models of groundwater flow: a case study of Gafsa mining basin-Southern Tunisia. *J. Afr. Earth Sci.*, 2014, **100**, 418–436.
- Candela, L., Elorza, F. J., Tamoh, K., Jiménez-Martínez, J. and Aureli, A., Groundwater modelling with limited data sets: the

- Chari–Logone area (Lake Chad Basin, Chad). *Hydrol. Process.*, 2014, **28**(11), 3714–3727.
12. Dahan, O., McGraw, D., Adar, E., Pohl, G., Bohm, B. and Thomas, J., Multi-variable mixing cell model as a calibration and validation tool for hydrogeologic groundwater modeling. *J. Hydrol.*, 2004, **293**(1–4), 115–136.
 13. Sanford, W. E., Plummer, L. N., Mcada, D. P., Bexfield, L. M. and Anderholm, S. K., Hydrochemical tracers in the middle Rio Grande Basin, USA: 2. Calibration of a groundwater-flow model. *Hydrogeol. J.*, 2004, **12**(4), 389–407.
 14. Mohammadi, Z., Salimi, M. and Faghieh, A., Assessment of groundwater recharge in a semi-arid groundwater system using water balance equation, southern Iran. *J. Afr. Earth Sci.*, 2014, **95**, 1–8.
 15. Hao, Q., Shao, J., Cui, Y. and Zhang, Q., Development of a new method for efficiently calculating of evaporation from the phreatic aquifer in variably saturated flow modeling. *J. Groundwater Sci. Eng.*, 2016, **4**(1), 26–34.
 16. Richards, L. A., Capillary conduction of liquids through porous mediums. *J. Appl. Phys.*, 1931, **1**(5), 318–333.
 17. Cui, Y., Su, C., Shao, J., Wang, Y. and Cao, X., Development and application of a regional land subsidence model for the plain of Tianjin. *J. Earth Sci.*, 2014, **25**(3), 550–562.
 18. Rui, X.-F., *Principles of Hydrology*, China Water Power Press, Beijing, 2004, pp. 114–118.
 19. Zhang, H. and Hiscock, K. M., Modelling the effect of forest cover in mitigating nitrate contamination of groundwater: a case study of the Sherwood Sandstone aquifer in the East Midlands, UK. *J. Hydrol.*, 2011, **399**(3–4), 212–225.
 20. Surinaidu, L., Bacon, C. G. D. and Pavelic, P., Agricultural groundwater management in the Upper Bhima Basin, India: current status and future scenarios. *Hydrol. Earth System Sci.*, 2013, **17**(1), 507–517.
 21. Pollock, D. W., User's Guide for MODPATH/MODPATH-PLOT, Version 3: A Particle Tracking Post-processing Package for MODFLOW, the US: Geological Survey Finite, 1994.
 22. Wu, Y., Wang, W., Toll, M., Alkhoury, W., Sauter, M. and Kolditz, O., Development of a 3D groundwater model based on scarce data: the Wadi Kafrein catchment, Jordan. *Environ. Earth Sci.*, 2011, **64**(3), 771–785.
 23. Gonçalves, T. D., Fischer, T., Gräbe, A., Kolditz, O. and Weiss, H., Groundwater flow model of the Pípiripau watershed, Federal District of Brazil. *Environ. Earth Sci.*, 2013, **69**(2), 617–631.
 24. Massoudieh, A., Visser, A., Sharifi, S. and Broers, H. P., A Bayesian modeling approach for estimation of a shape-free groundwater age distribution using multiple tracers. *Appl. Geochem.*, 2014, **50**, 252–264.
 25. Tóth, J., A theoretical analysis of groundwater flow in small drainage basins. *J. Geophys. Res.*, 1963, **68**(16), 4795–4812.
 26. Jiang, X. W., Wan, L., Wang, X. S., Ge, S. and Liu, J., Effect of exponential decay in hydraulic conductivity with depth on regional groundwater flow. *Geophys. Res. Lett.*, 2009, **36**(24), 88–113.

ACKNOWLEDGEMENTS. This research was supported by the Fundamental Research Funds for the Central Universities (2652016022), the Fundamental Research Funds for central public research institutes (YYWF201626), the project '1 : 50,000 hydrogeology survey in Bayin River & Tataling River Basin of the Qaidam Basin (DD20160291)' and 'hydrogeology and environmental geology survey in the circular economy pilot area of the Qaidam Basin (1212011220974)' by the China Geological Survey. We thank Qiulan Zhang and Yong Xiao for careful editing of the text and Ge Zhang, Feng Liu, Xinyue Tang, Yong Xiao for their field works.

Received 25 June 2016; revised accepted 22 March 2017

doi: 10.18520/cs/v113/i03/403-412